Biogeosciences, 10, 5061–5078, 2013
www.biogeosciences.net/10/5061/2013/
doi:10.5194/bg-10-5061-2013


Biogeosciences
Open Access

# Timing of fire relative to seed development may enable non-serotinous species to recolonize from the aerial seed banks of fire-killed trees

**S. T. Michaletz[1,2], E. A. Johnson[2], W. E. Mell[3], and D. F. Greene[4]**

[1]Department of Ecology and Evolutionary Biology, University of Arizona, 1041 E Lowell St., BSW #310, Tucson, AZ 85721, USA
[2]Department of Biological Sciences and Biogeoscience Institute, University of Calgary, 2500 University Drive NW, Calgary, AB T2N 1N4, Canada
[3]Pacific Wildland Fire Sciences Lab, US Forest Service, 400 N. 34th St. Suite 201, Seattle, WA 98103, USA
[4]Department of Geography, Planning & Environment, Concordia University, 1455 de Maisonneuve W., H 1255-26 Montreal, QC H3G 1M8, Canada

*Correspondence to:* S. T. Michaletz (michaletz@email.arizona.edu)

Received: 17 September 2012 – Published in Biogeosciences Discuss.: 22 November 2012
Revised: 17 June 2013 – Accepted: 23 June 2013 – Published: 26 July 2013

**Abstract.** The existence of non-serotinous, non-sprouting species in fire regimes where serotiny confers an adaptive advantage is puzzling, particularly when these species recruit poorly from soil seed banks or from burn edges. In this paper, white spruce (*Picea glauca* (Moench) Voss) was used to show how the timing of fire relative to seed development may permit non-serotinous species to recolonize burned areas from the aerial seed banks of fire-killed trees. To estimate survival of seeds within closed cones during crown fires, cone heating was simulated using a one-dimensional conduction model implemented in a three-dimensional computational fluid dynamics fire behavior model. To quantify the area burned when germinable seed would be contained within closed cones during a mast year, empirical fire occurrence and seed development (germinability and cone opening) data were compared for multiple locations across the white spruce range. Approximately 12 % of cones contained viable seed following crown fire simulations (0.072 $\mathrm{m\,s^{-1}}$ mean spread rate; 9147 $\mathrm{kW\,m^{-1}}$ mean intensity), and roughly half of the historical area burned resulted from fires that occurred when closed cones would contain germinable seed. Together, these results suggest that non-serotinous species may recolonize burned areas from in situ aerial seed banks, and that this may be an important cause of their existence in fire regimes to which they otherwise seem poorly suited.

## 1 Introduction

Serotiny is the retention of germinable seed within a parent plant crown for a period longer than the interval between successive seed cohorts (Le Maitre, 1985; Lamont et al., 1991). Fire can initiate seed release from all serotinous seed-bearing structures (but it is requisite for less than 5 % of serotinous species; Lamont et al., 1991). Serotiny is fire-adaptive for non-sprouting (obligate seeding) species in some fire regimes (Enright et al., 1998; Gill, 1981; Lamont and Enright, 2000; Keeley et al., 2011; Schwilk and Ackerly, 2001), as it not only provides a persistent aerial seed bank for post-fire recruitment but can also insulate seeds against heat necrosis via the thickened walls or clustering of seed-bearing structures (Mercer et al., 1994; Beaufait, 1960; Judd, 1993; Bradstock et al., 1994; Despain et al., 1996; Fraver, 1992). Theory suggests that serotiny should be favored when mean fire return intervals are longer than a species' time to reproductive maturity but shorter than its lifespan, and inter-fire recruitment is rare and/or unsuccessful at producing reproductively mature individuals (Enright et al., 1998; Lamont and Enright, 2000); conversely, non-serotiny should be favored when mean fire return intervals are longer than a species' lifespan and inter-fire recruits can survive to reproductive maturity.

Published by Copernicus Publications on behalf of the European Geosciences Union.

However, this theory does not explain why many non-serotinous species are also very common in such fire regimes. An example is white spruce (*Picea glauca* (Moench) Voss), which coexists with serotinous competitors jack pine (*Pinus banskiana* (Lamb.)), lodgepole pine (*Pinus contorta* Dougl. ex. Loud.), and black spruce (*Picea mariana* (Mill) B.S.P.), and is common throughout the North American boreal forest where mean fire return intervals (< 150 yr; Payette, 1992; Gauthier et al., 1996) are shorter than the lifespans of constituent tree species (Johnson, 1992). While inter-fire recruitment does occur for white spruce, it has little adaptive value as the recruits have a low probability of reaching reproductive maturity before the next fire event (Johnson et al., 1994, 2003; Youngblood, 1995; Gutsell and Johnson, 2002). Thus, the ubiquity of white spruce in the North American boreal forest is paradoxical, as the species should either be serotinous, or rare and relegated to small, unburned patches of old forest where inter-fire recruits could survive to reproductive maturity (Enright et al., 1998; Lamont and Enright, 2000).

Clearly, additional seed sources must account for the ubiquity of white spruce. Soil seed banks are not available, however, as they are limited by seed predation and temporal loss of viability (Johnson and Fryer, 1996; Nienstadt and Zasada, 1990), or are consumed by smoldering combustion of the upper organic soil horizons (Miyanishi, 2001). It has therefore been assumed that white spruce recruitment occurs via wind dispersal of seed from live sources on burn edges (including residual unburned areas within the fire; Galipeau et al., 1997; Wirth et al., 2008; Greene and Johnson, 2000). However, it is unlikely that dispersal alone is responsible for white spruce recruitment, as recruitment in high densities near burn edges requires fire during or soon before a mast year (Peters et al., 2005), and the large size of fires responsible for most of the area burned in the boreal forest (Johnson, 1992) imposes a dispersal constraint that would limit high densities of recruitment to areas within about 100 m of burn edges (Greene and Johnson, 2000).

We suggest another possibility: germinable seed contained within closed cones can survive fire to provide transient aerial seed banks (Thompson and Grime, 1979) for post-fire recruitment. Previous studies have shown that the onset of seed germinability begins well before the onset of cone opening, such that germinable seed is contained within closed cones for a considerable period of the growing season prior to seed abscission (Zasada, 1973, 1978; Winston and Haddon, 1981; Cram and Worden, 1957; Crossley, 1953). It is expected that these closed cones can insulate their seeds against heat necrosis during a fire, because white spruce cone diameter (and consequently the radial heat transfer characteristics; Incropera et al., 2006) is nearly identical to that of black spruce (Parker and McLachlan, 1978), and black spruce seeds generally have high rates of viability after fire (Lutz, 1956; Greene and Johnson, 1999). This suggests that the timing of fire relative to seed development (germinability and cone opening) governs the availability of aerial seed banks for white spruce in burned areas.

The objectives of this paper are as follows: (1) to use a physical process simulation approach to predict that seeds in closed cones can survive heating by crown fire, and (2) to demonstrate empirically that a large proportion of area burned occurs when germinable seed would be contained within closed cones. Cone heating in crown fires was simulated using a one-dimensional conduction model implemented in a three-dimensional computational fluid dynamics (CFD) model of forest fire behavior. These simulations are not intended to characterize the entire spectrum of variability in fire behavior that can occur across the range of white spruce, but are instead used to investigate if seeds in closed cones can survive heating by crown fire. Timings of fire and seed development were compared using historical fire occurrence and area burned data with seed germination studies from several locations across the range of white spruce. This is one of the first efforts to characterize the ecological effects of fire using a relatively complete model of physical fire processes (including heat transfer within vegetation). Although this analysis considers the example of white spruce in the North American boreal forest, the simulated processes are general to seed-bearing structures of other species, and the arguments should inform understanding of vegetation dynamics in other fire-prone areas.

## 2 A one-dimensional model of cone heating in forest fires

White spruce seeds are located around the longitudinal cone axis, with seed embryos located immediately adjacent to the axis (Fig. 1). In a forest fire, heat flux incident on the cone surface via radiation and convection is conducted in towards the longitudinal axis in response to radial temperature gradients. Endothermic thermal degradation reactions (evaporation and pyrolysis) limit the rate of temperature increase. However, seed necrosis can occur if embryos are heated to sufficiently high temperatures for sufficiently long periods of time.

White spruce cones have low Reynolds numbers (*Re*) and high length-to-radius ratios, so heat fluxes are relatively uniform around the cone circumference, and conduction occurs primarily in the radial direction. Leeward convective fluxes are not enhanced by turbulent eddy motion in this *Re* regime (Giedt, 1949), and the scales of closed cones are tightly sealed so there are no channels that could permit convection of hot gases from the exterior to the interior of the cone (Fig. 1). Consequently, cone heating can be characterized as one-dimensional conduction in cylindrical coordinates (Incropera et al., 2006; McGrattan et al., 2010a):

$$\rho_c c_c \frac{\partial T_c}{\partial t} = \frac{1}{r}\frac{\partial}{\partial r}\left(r k_c \frac{\partial T_c}{\partial r}\right) + \dot{q}''', \tag{1}$$

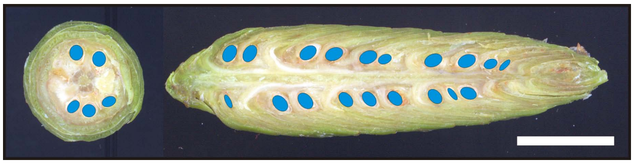

**Fig. 1.** White spruce cone anatomy in cross (left) and longitudinal (right) sections. Blue areas approximate the intersections of seeds and sections. For cones heated in a fire, radial conduction occurs from the cone surface towards the longitudinal cone axis. Scale bar represents 1 cm.

where $\rho_c$ is cone density (kg m$^{-3}$), $c_c$ is cone specific heat capacity (J kg$^{-1}$ K$^{-1}$), $k_c$ is cone thermal conductivity (W m$^{-1}$ K$^{-1}$),$T_c$ is cone temperature (°C), $t$ is time (s), and $r$ is radial position (m). A similar approach was used by Mercer et al. (1994) to study seed survival in woody fruits during fires. The energy source term $\dot{q}'''$ accounts for heat loss or gain per unit volume (W m$^{-3}$) via evaporation, pyrolysis, or combustion. The boundary condition along the longitudinal axis is

$$k_c \frac{\partial T_c}{\partial r} = 0, \tag{2}$$

and the boundary condition at the surface is

$$-k_c \frac{\partial T_c}{\partial r}(0,t) = \dot{q}''_{\text{conv}} + \dot{q}''_{\text{rad}}. \tag{3}$$

The convective flux $\dot{q}''_{\text{conv}}$ (W m$^{-2}$) is given by

$$\dot{q}''_{\text{conv}} = h\left(T_a - T_{\text{surf}}\right), \tag{4}$$

where $T_a$ (° C) is the temperature of air adjacent to the cone surface and $T_{\text{surf}}$ (°C) is the cone surface temperature. The convective heat transfer coefficient $h$ (W m$^{-2}$ K$^{-1}$) is taken as the greater of free and forced components (Holman, 1997; Incropera et al., 2006)

$$h = \max\left[C\,(\Delta T)^{1/3}, \left(\frac{k_a}{D}\right)\left(0.664\,Re^{1/2}\,Pr^{1/3}\right)\right], \tag{5}$$

where $C$ is a free convection coefficient (1.52 or 1.31 for horizontal or vertical surfaces, respectively), $D$ (m) is cone diameter, $k_a$(W m$^{-1}$ K$^{-1}$) is the thermal conductivity of air, and the Prandtl number $Pr$ (dimensionless) is the ratio of momentum and thermal diffusivities. The radiative flux $\dot{q}''_{\text{rad}}$(W m$^{-2}$) is given by

$$\dot{q}''_{\text{rad}} = \varepsilon_c \dot{q}''_i - \varepsilon_c \sigma T^4_{\text{surf}}, \tag{6}$$

where $\varepsilon_c$ is the cone emissivity (dimensionless), $\dot{q}''_i$ (W m$^{-2}$) is the radiative heat flux incident from the fire and plume to the cone surface, and $\sigma$ is the Stefan–Boltzmann constant ($5.67 \times 10^{-8}$ W m$^{-2}$ K$^{-4}$).

## 3 Materials and methods

### 3.1 Cone collection

Cones used for model parameterization (Eqs. 1–6) and germination studies (see below) were collected during the summers of 2006 and 2010. During 2006, cones for germination studies were collected between 23 July and 1 September (757.35 to 1121.19 accumulated degree days) from a mature white spruce stand in Kananaskis Country, Alberta, Canada (51°01′32″ N, 114°52′22″ W; Fig. 2). Accumulated degree days (beginning ordinal day 1) were calculated using the double-sine method with a lower threshold of 5 °C (Allen, 1976; Zasada, 1973) and maximum and minimum daily temperature data obtained from the Barrier Lake Station of the Biogeoscience Institute of the University of Calgary (11.33 km away from the collection site). Each week, five randomly chosen trees were felled and approximately 100 cones were collected from each. Cones were placed in paper bags and transported to the laboratory, where they were stored at approximately 22 °C until the date of natural cone opening (Zasada, 1973, 1978); cone drying thus occurred in a manner similar to the drying of cones on a dead tree following a forest fire. Seed extraction and germination studies began once the scales reflexed on cones from the last sampling date (see below). During 2010, cones for model parameterization and germination studies were collected between 14 June and 9 September (345.32 to 1221.27 accumulated degree days) from open-grown trees at the University of Calgary campus in Calgary, Alberta, Canada (51°04′49″ N, 114°07′27″ W; Fig. 2). Accumulated degree days were calculated as above using temperature data from the Calgary International Airport (8.16 km from the collection site; http://climate.weatheroffice.gc.ca). Each week, five cones were sampled from each of five trees that had been selected on the first sampling date. Cones were transported to the laboratory, where four cones from each tree were stored and processed as described for the 2006 cones, and one cone from each tree was enclosed in a plastic zipper bag and frozen at −22.4 °C for measurement of physical properties for the cone heat transfer model (see below).

### 3.2 Simulation of cone heating by crown fire

Cone heating and crown fire spread were simulated using the Wildland–Urban Interface Fire Dynamics Simulator (WFDS), which is a joint product of the US Forest Service and the National Institute of Standards and Technology (NIST). The WFDS is a CFD model of fire spread through thermally thin vegetative fuels, which provide momentum drag and heat and mass fluxes to the fluid (Mell et al., 2009, 2007). The model is an extension of the NIST Fire Dynamics Simulator 6 (FDS), which numerically solves Navier–Stokes approximations that are appropriate for the low-velocity, thermally driven flows characteristic of fires


**Fig. 2.** Map showing the range of white spruce (Little, 1971) with cone collection locations, weather station locations, germination study locations, and forest fire observation areas.

(McGrattan et al., 2010b; Rehm and Baum, 1978). An explicit predictor–corrector scheme (second-order accurate in space and time) is used to march the solution forward in time through a three-dimensional rectilinear grid. Turbulence is modeled by large eddy simulation (LES), which resolves flow at scales larger than the grid cell size and parameterizes flow at subgrid scales (direct numerical simulation may also be used with grid cells of sufficiently fine resolution). Fluid flow solutions are coupled with solid-phase evaporation and pyrolysis models, a gas-phase mixture fraction combustion model, and a radiation transport equation solver. Time steps may vary throughout the simulation to satisfy the Courant–Friedrichs–Lewy condition (McGrattan et al., 2010a). Detailed descriptions of the WFDS and the FDS are given in Mell et al. (2007, 2009) and McGrattan et al. (2010a).

The one-dimensional conduction model used to characterize cone heating (Eqs. 1–6) is implemented within WFDS. For every WFDS time step, cone temperatures were updated using the implicit Crank–Nicolson method (cf. Chapra and Canale, 2009), which is second-order accurate in space and time. Node spacing was uniform and chosen to satisfy

$$\delta r < \sqrt{\frac{k_c}{\rho_c c_c}}. \tag{7}$$

The conduction model is coupled to WFDS via the boundary condition described in Eq. (3); convective flux $\dot{q}''_{\mathrm{conv}}$ (Eq. 4) is calculated from properties of the cone surface ($T_{\mathrm{surf}}$) and the gas adjacent to the cone surface ($T_{\mathrm{a}}$, $Re$, and $Pr$), whereas radiative flux $\dot{q}''_{\mathrm{rad}}$ (Eq. 6) is based on solution of the radiation transport equation. Additional details on the conduction model, numerical scheme, and coupling to WFDS can be found in McGrattan et al. (2010a).

The FDS has undergone extensive validation (McGrattan et al., 2010b; McDermott et al., 2010), and the WFDS extension has been validated for fire spread through grasslands (Mell et al., 2007) as well as the burning of individual tree crowns (Mell et al., 2009). The one-dimensional conduction model and Crank–Nicolson scheme have been validated using analytical solutions of the conduction equation (McDermott et al., 2010) and heating experiments with cylindrical geometries (electrical cables; McGrattan, 2008). The WFDS is increasingly being used as a physics-based "laboratory" for conducting experiments on fire spread through vegetation (Mell et al., 2009, 2007; Parsons et al., 2011; Hoffmann et al., 2012).

Parameter values used for the cone heating model are shown in Table 1. Physical properties were measured using the cones collected during 2010. In preliminary cone heating simulations, maximum seed temperatures varied less than 10 % between the first and last sampling dates (345.32 and 1221.27 degree days, respectively; Supplement Fig. A1), so means calculated during the entire 2010 sampling period

**Table 1.** Parameter values used for the cone heat transfer model (Eqs. 1–6)*.

| Definition | Symbol | Value (units) | Source |
|---|---|---|---|
| Char fraction | $\chi_{\text{char}}$ | 0.234 (dimensionless) | Grønli et al. (2002) |
| Density, char | $\rho_{\text{char}}$ | 46.31 $\text{kg m}^{-3}$ | Ragland et al. (1991) |
| Density, dry cone | $\rho_{\text{dc}}$ | 308.712 $\text{kg m}^{-3}$ | Measured |
| Density, water | $\rho_{\text{w}}$ | 997 $\text{kg m}^{-3}$ | Incropera et al. (2006) |
| Depth, seed | $r_{\text{s}}$ | 0.005 m | Measured |
| Diameter, cone | $D$ | 0.013 m | Measured |
| Emissivity, char | $\varepsilon_{\text{char}}$ | 0.95 (dimensionless) | Gupta et al. (2003) |
| Emissivity, cone | $\varepsilon_{\text{c}}$ | 0.94 (dimensionless) | Measured |
| Heat of combustion | $\Delta h_{\text{c}}$ | 17 936 $\text{kJ kg}^{-1}$ | Mell et al. (2009), Susott (1982b) |
| Heat of pyrolysis | $\Delta h_{\text{pyr}}$ | 418 $\text{kJ kg}^{-1}$ | Morvan and Dupuy (2004) |
| Heat of vaporization | $\Delta h_{\text{vap}}$ | 2257 $\text{kJ kg}^{-1}$ | Incropera et al. (2006) |
| Length, cone | $l$ | 0.044 m | Measured |
| Mass fraction, dry cone | $\chi_{\text{dc}}$ | 0.31 | Measured |
| Mass fraction, water | $\chi_{\text{w}}$ | 0.69 | Measured |
| Specific heat, char | $c_{\text{char}}$ | $c_{\text{char}} = 3.8 \times 10^{-6} T^2 + 0.004T + 0.555\,\text{kJ kg}^{-1}\,^\circ\text{C}^{-1}$ | Gupta et al. (2003) |
| Specific heat, dry cone | $c_{\text{dc}}$ | $c_{\text{dc}} = 1.16 + 3.867 \times 10^{-3} T\ \text{kJ kg}^{-1}\,^\circ\text{C}^{-1}$ | Simpson and TenWolde (1999) |
| Specific heat, water | $c_{\text{w}}$ | $c_{\text{w}} = -5 \times 10^{-11} T^5 + 2 \times 10^{-8} T^4 - 2 \times 10^{-6} T^3$ $+1 \times 10^{-4} T^2 - 3.5 \times 10^{-3} T + 4.217\,\text{kJ kg}^{-1}\,^\circ\text{C}^{-1}$ | Incropera et al. (2006) |
| Temperature, boiling | | 100 °C | Incropera et al. (2006) |
| Temperature, pyrolysis | | 200 °C | Susott (1982a) |
| Thermal conductivity, char | $k_{\text{char}}$ | 0.095 $\text{W m}^{-1}\,^\circ\text{C}^{-1}$ | Gupta et al. (2003) |
| Thermal conductivity, dry cone | $k_{\text{dc}}$ | $k_{\text{dc}} = 0.085 + 2.25 \times 10^{-4} T\ \text{W m}^{-1}\,^\circ\text{C}^{-1}$ | Simpson and TenWolde (1999) |
| Thermal conductivity, water | $k_{\text{w}}$ | $k_{\text{w}} = -7 \times 10^{-6} T^2 + 0.002T + 0.570\,\text{W m}^{-1}\,^\circ\text{C}^{-1}$ | Incropera et al. (2006) |

* Measured properties are means calculated over 757.35 to 1121.19 accumulated degree days.

(Table 1) were used for subsequent simulations. To measure physical properties, cones were removed from −22.4 °C storage and allowed to warm to approximately 22 °C. Fresh mass, length, diameter, and volume (via mass displacement of water) were measured for each cone. Longitudinal sections (Fig. 1) were used to measure seed depth (defined as embryo depth). Dry mass was measured after oven-drying at 95 °C to a constant mass. Bulk density was calculated from dry mass and fresh volume, and the mass fractions of water and dry cone (cellulose) were calculated from fresh and dry masses. Variation in physical properties throughout the sampling period was consistent with existing data for white spruce cones from Chalk River, Ontario (Winston and Haddon, 1981; Supplement Fig. B1). Thermal properties (Table 1) were obtained from the literature. Specific heat capacities $c$ and thermal conductivities $k$ of cone constituents (i.e., char, cellulose, and water) varied with temperature (Table 1), and the density $\rho_{\text{c}}$, specific heat capacity $c_{\text{c}}$, and thermal conductivity $k_{\text{c}}$ (Eq. 1) of the composite cone varied with simulated time in accordance with varying temperature and mass fractions of char, cellulose, and water (simple rule of mixtures). Cone char fraction was taken as that of *Picea abies* wood (Grønli et al., 2002). For char, density was taken as 15 % of dry cone density (Ragland et al., 1991), emissivity was taken as that of wood char (Gupta et al., 2003), and specific heat and thermal conductivity were taken as that of softwood char (Gupta et al., 2003). For dry cone, heat of combustion ($\text{kJ kg}^{-1}$ of *gaseous* fuel, Mell et al. (2009)) was taken as the mean of values reported for conifer foliage, wood, and bark (Susott, 1982b); heat of pyrolysis was taken as that of wood (Morvan and Dupuy, 2004); pyrolysis temperature was taken as that of forest fuels (Susott, 1982a); and specific heat and thermal conductivity were taken as that of white spruce wood (Simpson and TenWolde, 1999). For water, handbook values were used for density, specific heat, and thermal conductivity (Incropera et al., 2006).

Cone heating in crown fires was simulated in five 102 m × 50 m × 40 m computational domains at a resolution of 0.50 m × 0.50 m × 0.25 m (Fig. 3). Each simulation comprised 3.264 million grid cells, and 2000 s of simulated time required between 58 and 69 h on 48 3.0 GHz Intel® Xeon® X5450 processors. Although the computational grid cells were much larger than the cone diameter (0.013 m; Table 1), test simulations showed that the simulated seed temperatures were insensitive to oscillations of the net incident heat flux with frequencies that could potentially occur in a higher-resolution grid (Supplement C). Thus, if the simulations were run with a finer grid, resulting in heat flux time histories with higher-frequency components (all else being the same), the thermal response of the cone would be unchanged. In fact, as shown in Supplement C, the grid resolution used for the reported crown fire simulations are capable

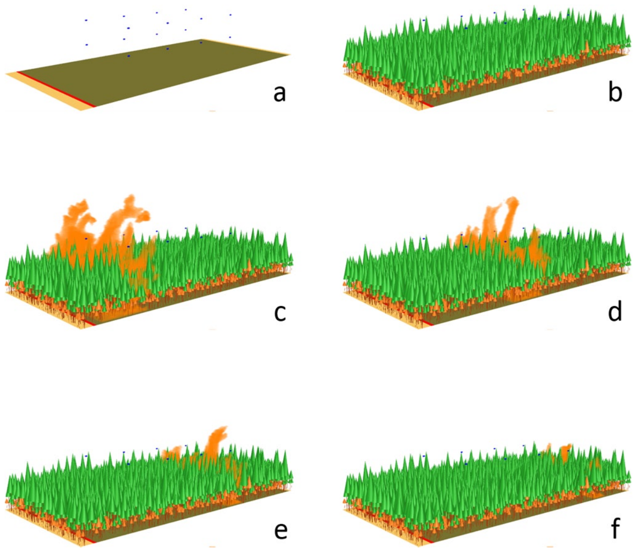


**Fig. 3.** Example of computational domains, cone locations **(a)**, forest canopy structure **(b–f)**, and visualization of WFDS output at $t = 0$ s **(b)**, $t = 250$ s **(c)**, $t = 500$ s **(d)**, $t = 750$ s **(e)**, and $t = 1000$ s **(f)**. Blue ellipsoids (not to scale) represent cone locations, green crowns represent live trees, and orange crowns represent dead trees. Smoke plume is not shown.

of resolving fluctuations in the heat flux with frequencies that are above the cone's response threshold. A mature, closed-canopy white spruce forest was generated within each domain (Fig. 3) using forest inventory data, allometry models, and thermophysical properties from the literature (see below). For each simulation, 6259 independent random points (trees) were uniformly distributed across the 102 m × 50 m area using the runifpoint function from the package spatstat (Rolf and Adrian, 2005) in the statistical software R (R Development Core Team, 2011); thus, the five simulations shared a common size–frequency distribution, but each had a unique spatial arrangement of trees. Aside from differences in the spatial locations of trees, the simulations were identical. A homogeneous surface fuel bed (see below) was positioned on the $z = 0$ plane between $x = 5$ to 100 m and $y = -25$ to 25 m, and an ignition source (500 kW m$^{-2}$ for 70 s) was positioned on $z = 0$ between $x = 4$ to 5 m and $y = -25$ to 25 m (Supplement Fig. D1). White spruce cones were positioned in vertical arrays located at $x = 25.5$, 42.5 m, 59.5 m, and 76.5 m along $y = -12.5$ and 12.5 m planes (Figs. 3 and Supplement Fig. D1); cones were positioned at heights $z = 8.7$ and 17.7 m, which roughly bound the range within which most cones would be present in this canopy (Boggs et al., 2008; Greene et al., 2002). Open boundaries were located on the $x = 102$ and $z = 40$ m planes, an inflow boundary was located on the $x = 0$ m plane, and mirror boundaries were located on the $y = -25$ and 25 m planes. A time-averaged wind profile (Albini and Baughman, 1979; Supplement Fig. E1) was prescribed at the inflow boundary $x = 0$ according to

$$\bar{U}(z) = \max\left[\left(\frac{U_*}{K}\right)\ln\left(\frac{z-0.64H}{0.13H}\right), \frac{0.306U_{\mathrm{ref}}}{\sqrt{fH}\ln\left(\frac{10+0.36H}{0.13H}\right)}\right], \quad (8)$$

where $K$ is the von Kármán constant (0.41; dimensionless), $z$ is height (m), and $H$ is the maximum canopy height (17.7 m). $U_{\mathrm{ref}}$ is the wind velocity at the reference height $z_{\mathrm{ref}} = 27.7$ m (10 m above canopy height; Lawson and Armitage, 2008); $U_{\mathrm{ref}}$ was taken as 10 m s$^{-1}$. The volume-filling fraction $f$ (dimensionless) was taken as 0.12, which gives the same ratio of canopy velocity to reference velocity $U_c/U_{\mathrm{ref}}$ (Albini and Baughman, 1979) that was observed in a *Picea* stand (Norum, 1983) having the same percent crown closure (80 %) as the forest inventory data used to generate the forest canopy structure (see below). The friction velocity $U_*$ is given by (Monteith and Unsworth, 2008; Albini and Baughman, 1979)

$$U_* = \frac{U_{\mathrm{ref}}K}{\ln\left(\frac{z_{\mathrm{ref}}-0.64H}{0.13H}\right)}. \quad (9)$$

In all simulations, ignition occurred at 100 s to allow this inflow wind profile to establish steady-state air flow within the domain (Supplement Fig. F1).

The mirror conditions prevent flow across $y = -25$ and 25 m boundaries, which restricts flow in the $y$ direction. This can lead to higher $u$ velocities, rates of spread, and fire intensities as compared to cases with open boundaries. To quantify these effects, rate of spread and mean fire intensity for a 102 m × 50 m × 40 m domain with mirror boundaries at $y = -25$ and 25 m were compared to those for a 153 m × 75 m × 60 m domain with open boundaries at $y = -25$ and 25 m. Rates of spread and intensities were compared for $x = 5$ to 50 m because the fire stopped crowning at approximately $x = 50$ m for the case with open boundaries. Rate of spread $R$ (m s$^{-1}$) was estimated as

$$R = \frac{x_2 - x_1}{t_2 - t_1}. \quad (10)$$

Mean global fire intensity $\bar{I}$ (kW m$^{-1}$) was calculated as

$$\bar{I} = \frac{\sum_{i=1}^{n}\left(\frac{\dot{Q}_i}{L}\right)}{n}, \quad (11)$$

where $\dot{Q}_i$ is the total heat release rate (kW) at time step $i$, $L$ is the fireline length in the $y$ direction (50 m), and $n$ is the number of time steps. Here, $i = 1$ corresponds to the time step when the surface fire front reached $x = 5$ m, and $n$ corresponds to the time step when the surface fire front reached $x = 50$ m. Rate of spread and fire intensity were 1.71 and 2.52 times greater, respectively, for the case with mirror boundaries.

Canopy structure was generated from forest inventory data and allometric fuel biomass models. Forest inventory data for a mature white spruce stand with 80 % crown closure were obtained from site WS 04 of Ottmar and Vihnanek (1998; Table 2). Data did not include crown base height CBH of dead trees, so this was estimated as

$$\mathrm{CBH_{dead}} = Z - \mathrm{CR}(Z), \tag{12}$$

where $Z$ is total tree height and CR is the crown ratio (dimensionless) of live trees in the same DBH size class

$$\mathrm{CR} = \frac{Z - \mathrm{CBH_{live}}}{Z}. \tag{13}$$

Forest canopies comprised four DBH size classes, each having a constant DBH, height, and crown base height defined as size class means from Table 2. Individual tree crowns were modeled as cones (Mell et al., 2009) using height and crown base height data from Table 2 with crown width $w$ (m) estimates from an ordinary least-squares regression of log-transformed data for *P. englemannii* ($R^2 = 0.888$; Brown, 1978):

$$w = 0.797\mathrm{DBH}^{0.444}. \tag{14}$$

The physical properties of crown fuels are given in Tables 3 and 4. For each DBH size class, crown fuel masses were estimated from allometric equations for suppressed trees (DBH $\leq$ 5.1 cm; Woodard and Delisle, 1987) and codominant/dominant trees (DBH > 5.1 cm; Johnson et al., 1990). Four crown fuel size classes were considered: foliage, 0–0.5 cm roundwood, 0.5–1.0 cm roundwood, and 1.0–3.0 cm roundwood. All crown fuels $\leq$ 1.0 cm diameter were considered available for combustion, since these diameters were completely consumed in tree-burning experiments and mass-loss rates were best predicted by WFDS with inclusion of these diameters (Mell et al., 2009). The 1.0–3.0 cm roundwood class was not available for combustion, but was included as a source of radiation absorption and momentum drag. The bulk density of each size class (Table 3) was calculated as the quotient of fuel mass and crown volume (calculated for conical geometries, as above). Bulk densities varied with DBH (Table 3) due to DBH-dependent variation in fuel masses (Johnson et al., 1990; Woodard and Delisle, 1987) and crown volumes (Eq. 14); all other physical properties of crown fuels (Table 4) were constant with DBH. The surface-area-to-volume ratio of white spruce foliage was calculated from data of Michaletz and Johnson (2006). Surface-area-to-volume ratios of the roundwood size classes were estimated using white spruce branches growing in a closed canopy forest at the University of Calgary Biogeoscience Institute Barrier Lake Field Station in the southern Canadian Rocky Mountains of Alberta, Canada; values were calculated from length and diameter measurements of 20 branches per size class that were randomly chosen from the crowns of 20 individual trees. Water content of foliage was taken as the minimum value observed for white spruce after 600 accumulated degree days (Chrosciewicz, 1986); degree days were calculated as above using daily temperature data from 1974 at Slave Lake, Alberta (http://climate.weatheroffice.gc.ca). Water contents for live roundwood were obtained from Titus et al. (1992), and water contents for dead roundwood were taken as those typical of 1- (0–0.5 cm roundwood) and 10-hour (0.5–1 and 1.0–3.0 cm roundwood) fuels during crown fires (Rothermel, 1991). Char fraction of foliage was taken as the mean of conifer foliage values reported by Susott (1982b), and char fraction of roundwood was taken as the value for *P. abies* wood reported by Grønli et al. (2002). Particle density of foliage was obtained from Michaletz and Johnson (2006), and particle density of wood was calculated using relationships from Simpson and TenWolde (1999; assuming 0 % water content). For all crown fuels, emissivity was taken as 0.9 (Mell et al., 2009), heat of combustion was calculated as above (Table 1), maximum dehydration and burning rates were taken as 0.4 kg $\mathrm{s^{-1}\,m^{-3}}$ (Mell et al., 2009), and the drag force factor was taken as 3/8 (Mell et al., 2007, 2009; Morvan and Dupuy, 2001, 2004; Linn et al., 2002).

**Table 2.** Forest inventory data used to generate the white spruce canopy used in model simulations.

| DBH size class (cm) | Status | DBH (cm) | Density (ha$^{-1}$) | Crown base height (m) | Crown width (m) | Height (m) |
|---|---|---|---|---|---|---|
| $\leq$ 5.1 | live | 3.3 | 1327 | 3.30 | 1.35 | 5.3 |
| | dead | 2.5 | 3316 | 2.43 | 1.20 | 3.9 |
| 5.1–10.2 | live | 7.6 | 2777 | 5.20 | 1.96 | 8.7 |
| | dead | 6.4 | 250 | 4.02 | 1.82 | 6.8 |
| 10.2–22.9 | live | 13.5 | 1908 | 6.60 | 2.53 | 12.6 |
| | dead | 10.9 | 42 | 5.29 | 2.30 | 10.1 |
| > 22.9 | live | 25.1 | 208 | 6.90 | 3.34 | 17.7 |

Surface fuels were modeled using the vegetation boundary fuel method in WFDS. Fuel data typical of 100 to 200 yr old closed white spruce stands with feathermoss understories (Viereck et al., 1992) were obtained from fuel bed 101 of the Fuel Characteristic Classification System 2.1 (FCCS 2.1; Ottmar et al., 2007). Fuels comprised 1-hour woody fuels, 10-hour woody fuels, feathermosses, ladder fuels, lichen, litter, white spruce saplings (height $\leq$ 1.4 m), dead primary shrubs (*Alnus viridis* ssp. *crispa*, *Betula nana*, and *Salix* spp.; height $\leq$ 4.6 m), and dead secondary shrubs (*Empetrum nigrum*, *Ledum groenlandicum*, *Linnaea borealis*, *Vaccinium ulginosum*, and *Vaccinium vitis-idaea*; height $\leq$ 0.6 m). Surface fuels are listed in Table 5 along with their physical properties required for parameterization of the WFDS vegetation boundary fuel model. These physical properties were combined into a single homogeneous fuel bed following Rothermel's (1972) surface-area-weighting approach, modified to include Albini's (1976) revisions and Wilson's (1980) SI unit conversions; characteristic values for the homogeneous

**Table 3.** Crown fuel bulk densities (kg m$^{-3}$) used in model simulations*.

| DBH size class (cm) | Status | Crown fuel size class: Foliage | 0–0.5 cm roundwood | 0.5–1.0 cm roundwood | 1.0–3.0 cm roundwood |
|---|---|---|---|---|---|
| ≤ 5.1 | live | 0.332 | 0.141 | 0.038 | 0.154 |
| | dead | n/a | 0.131 | 0.040 | 0.125 |
| 5.1–10.2 | live | 1.850 | 1.150 | 0.299 | 0.363 |
| | dead | n/a | 1.236 | 0.330 | 0.372 |
| 10.2–22.9 | live | 1.249 | 1.193 | 0.286 | 0.449 |
| | dead | n/a | 1.200 | 0.297 | 0.423 |
| > 22.9 | live | 0.814 | 1.236 | 0.270 | 0.560 |

* n/a = not applicable.

**Table 4.** Physical properties of the four crown fuel size classes used in model simulations*.

| Crown fuel size class | Status | Char fraction (dimensionless) | Particle density (kg m$^{-3}$) | Surface-area-to-volume ratio (m$^{-1}$) | Water content (dimensionless) |
|---|---|---|---|---|---|
| Foliage | live | 0.260 | 628 | 4239.29 | 1.220 |
| 0–0.5 cm roundwood | live | 0.234 | 410 | 1434.66 | 0.781 |
| | dead | 0.234 | 410 | 1434.66 | 0.050 |
| 0.5–1.0 cm roundwood | live | 0.234 | 410 | 529.65 | 0.781 |
| | dead | 0.234 | 410 | 529.65 | 0.06 |
| 1.0–3.0 cm roundwood | live | n/a | 410 | 188.79 | n/a |
| | dead | n/a | 410 | 188.79 | n/a |

* The 1.0–3.0 cm size class was included as a source of radiation absorption and momentum drag only (combustion was not considered). Water content and char fraction are not listed for 1.0–3.0 cm fuels as these could not combust in model simulations. n/a = not applicable.

fuel bed are given in Table 5. It was assumed that all fuels ≤ 1.0 cm diameter were available for combustion (see above; Mell et al., 2009); consequently, loadings of feathermosses, lichen, litter, white spruce saplings, and primary and secondary shrubs were obtained directly from FCCS data, whereas loadings for 10 h and ladder fuels ≤ 1.0 cm diameter were estimated from FCCS data assuming a uniform distribution of fuel mass among diameters (20 and 39 % of total loadings of 10-hour and ladder fuels, respectively). Fuel depths for feathermosses, lichen, and litter were taken from FCCS data, and depths for white spruce saplings and woody fuels were assumed to be equal to the largest diameter of the fuel category (i.e., 1 cm; Keane and Dickinson, 2007). Char fractions were obtained from Susott (1982b); values for moss and lichen were taken as that of feathermosses, values for woody fuels were taken as the mean of conifer wood and bark, and the value for litter was taken as the mean of all conifer foliage. Particle densities of 1-hour, 10-hour, and ladder fuels were calculated as above (Simpson and TenWolde, 1999), particle density of litter was obtained from Michaletz and Johnson (2006), and the mean of these values was used for white spruce saplings. Particle densities of moss and lichen were calculated as the quotient of feathermoss bulk density and packing ratio (O'Donnell et al., 2009), and particle densities of primary and secondary shrubs were calculated as the mean of *Salix* spp. wood (Singh, 1987) and foliage (quotient of leaf-specific mass and leaf thickness; Koike, 1988). Surface-area-to-volume ratios for 1- and 10-hour fuels were taken as those measured for crown fuels (described above), for moss and lichen as the value measured for feathermosses by Sylvester and Wein (1981), for ladder fuels as the mean of 1- and 10-hour fuels (see above), for white spruce saplings as the mean of measured 1- and 10-hour fuels and foliage (Michaletz and Johnson, 2006), and for litter as the value for white spruce foliage (Michaletz and Johnson, 2006). Water content of white spruce saplings was taken as the mean of live foliage and branches (see above), and water contents of all other fuels were taken as those typical of 1- and 10-hour fuels during crown fires (as above; Rothermel, 1991). Heat of combustion, specific heat, and emissivity were taken as above for crown fuels. Maximum mass-loss rate can affect rate of spread and should ideally be measured for the fuel bed under consideration; since these data were not available for the fuel bed used here, this parameter was instead adjusted to 0.42 kg s$^{-1}$ m$^{-3}$ so that simulated rates of spread roughly agreed with observations from North American *Picea* stands

Table 5. Fuel types, categories, and physical properties used to generate the homogeneous surface fuel bed used in model simulations.

| Type | Category | Bed depth (m) | Char fraction (dimensionless) | Loading ($kg\,m^{-2}$) | Particle density ($kg\,m^{-3}$) | Surface-area-to-volume ratio ($m^{-1}$) | Water content (dimensionless) |
|---|---|---|---|---|---|---|---|
| 1-hour woody | Woody | 0.01 | 0.266 | 0.07 | 410 | 1434.66 | 0.06 |
| 10-hour woody* | Woody | 0.01 | 0.266 | 0.02 | 410 | 529.65 | 0.07 |
| Feathermosses | Moss | 0.064 | 0.355 | 0.59 | 1818.18 | 25 000 | 0.06 |
| Ladder fuels* | Woody | 0.01 | 0.266 | 0.04 | 410 | 982.15 | 0.07 |
| Lichen | Lichen | 0.051 | 0.355 | 0.01 | 1818.18 | 25 000 | 0.06 |
| Litter | Litter | 0.025 | 0.286 | 0.67 | 628.11 | 4239.29 | 0.06 |
| White spruce saplings | Live | 0.01 | 0.274 | 0.01 | 519.06 | 2478.34 | 0.87 |
| Primary shrubs | Woody | 0.01 | 0.266 | 0.40 | 622.77 | 746.85 | 0.06 |
| Secondary shrubs | Woody | 0.01 | 0.266 | 1.20 | 622.77 | 746.85 | 0.06 |
| Homogeneous fuel bed | n/a | 0.045 | 0.323 | 3.01 | 1296.44 | 15 048 | 0.06 |

* Properties pertain to $D \leq 1$ cm.
n/a = not applicable.

(Norum, 1982; Kiil, 1975; Alexander et al., 1991). We note that while these stands do not conform exactly to the stands considered in this study (i.e., 17.7 m white spruce stands with 80 % crown closure), they are the only data we are aware of that describe fire spread rates in North American *Picea* stands. We further note that adjustment of the maximum mass-loss rate parameter can yield different rates of spread. The drag force factor was taken as 0.1(3/8), which accounts for the approximate 1 : 10 ratio of fuel bed height to grid cell height (Mell et al., 2007, 2009; Morvan and Dupuy, 2001, 2004; Linn et al., 2002).

Five simulations were conducted, each containing 16 cones. Each simulation had a unique spatial arrangement of trees, but all simulations shared a common size–frequency distribution (see above). For each simulation, rate of spread (Eq. 10) and mean fire intensity (Eq. 11) were calculated for $5 \leq \times \leq 95$ m; note that for each simulation, fire spread was not steady-state, and both rate of spread and intensity varied through time and space. Time steps for the CFD and one-dimensional conduction model varied between an initial value of 0.099 s and a minimum value of 0.00354 s. The radius of each cone was divided into 20 nodes spaced every 0.00037 m. For each cone, surface temperature, seed temperature, total convective heat flux, and total radiative heat flux were recorded every 1 s. Time-integrated total heat fluxes were calculated for each cone by summing (since $\Delta t = 1$ s) total convective and radiative heat fluxes. The necrosis kinetics of white spruce seeds have not been established, so cones from all simulations were combined and the cumulative proportion of cones containing viable seed $\hat{F}_N(T_n)$ was plotted as a function of threshold necrosis temperature $T_n$:

$$\hat{F}_N(T_n) = \frac{\text{number of cones with } T_{max} \leq T_n}{\text{total number of cones}} = \frac{1}{N}\sum_{i=1}^{N} 1\left\{T_{max,i} \leq T_n\right\}, \quad (15)$$

where $T_{max}$ is the maximum seed temperature of each cone $i$, $N$ is the total number of cones ($N = 80$), and $1\left\{T_{max,i} \leq T_n\right\}$ is the indicator of $T_{max} \leq T_n$. This approach is useful given the lack of necrosis kinetics data, as it permitted estimation of the proportion of cones containing viable seeds $\hat{F}_N(T_n)$ for any seed necrosis temperature. Here we assume a threshold necrosis temperature of 70 °C, which was observed for non-stratified *Picea abies* (Norway spruce) seeds subjected to a 10 min exposure (Granström and Schimmel, 1993). In reality, the threshold necrosis temperature is probably higher because exposure times are lower for seeds in cones heated by forest fires (maximum of approximately 3 min; see Sect. 5).

### 3.3 Timing of fire occurrence and seed development

The timing of fire occurrence and seed development (germinability and cone opening) was examined for multiple locations across the range of white spruce (Fig. 2). Timing of fire occurrence was estimated using climate and fire data for Canada and Alaska from 1959 to 2009. Climate (daily temperature) data were obtained from Environment Canada (http://climate.weatheroffice.gc.ca) and the National Ocean and Atmospheric Administration National Climatic Data Center (http://www.ncdc.noaa.gov). Data for each year were available for Jasper and Yellowknife, but at other locations data were missing for 1 to 4 yr (Bagotville, Fairbanks, Fort Smith, and Sioux Lookout), 8 yr (Schefferville), and 11 yr (La Ronge). For each annual record, accumulated degree days were calculated as above; these data were then used to calculate the mean accumulated degree days for each ordinal day at each site. Fire data from Canada and Alaska were obtained from the Canadian National Fire Database (formerly the Canadian Large Fire Database, Stocks et al., 2002; http://cwfis.cfs.nrcan.gc.ca/nfdb) and the Bureau of Land Management Alaska Fire Service (http://fire.ak.blm.gov/predsvcs/maps.php). Data were truncated to include only lightning fires $\geq 200$ ha that originated within 2° latitude × 2° longitude "fire observation areas" centered around weather stations used for degree day calculations (except for Yellowknife, where the area was centered 1° north of the station to avoid Great Slave Lake). For each fire observation area, the area burned per ordinal day was estimated by assuming a steady-state rate of spread between fire start and end dates; although this is an unrealistic assumption, it provides a better estimate of area burned per day than do fire start or end dates alone (which would necessarily assume that all area burned occurs on the day of ignition or extinction). Start dates were available for all fires in all fire observation areas. End dates were available for some fires at Fairbanks, Fort Smith, La Ronge, and Sioux Lookout; for these areas, fires without end dates were excluded from the analysis. End dates were not available for fires at Bagotville, Jasper, Schefferville, and Yellowknife, so they were estimated using a backwards stepwise multiple regression equation ($F_{13,2558} = 49.53$, $P < 2.2 \times 10^{-16}$, $R^2 = 0.2011$) based on data from all fires in Canada for which start and end dates were available ($N = 2572$); area burned, latitude, longitude, start date, and year were used as explanatory variables because they characterize the processes controlling fuel drying, ignition, rate of spread, and extinction (Macias Fauria et al., 2011; Macias Fauria and Johnson, 2006; Johnson, 1992). Timing of fire occurrence was expressed as the cumulative distribution

$$\hat{S}(t) = \frac{\text{area not yet burned}}{\text{total area burned}} = \frac{1}{A_{\text{total}}} \sum_{i=1}^{n} A_i 1\{t_i > t\}, \qquad (16)$$

where $t$ is ordinal day (in accumulated degree days), $A_{\text{total}}$ is the total area burned, $n$ is the total number of ordinal days, $A_i$ is the area burned on ordinal day $i$, and $1\{t_i > t\}$ is the indicator of $t_i > t$.

Timing of seed development was estimated using germination studies of seeds from cones collected at Kananaskis Country during 2006 and Calgary during 2010 (see above; Fig. 2). Seed extraction occurred after the last sampling date (i.e., date of cone opening), by which time previously collected cones had dried and cone scales had reflexed open. Mechanical shaking was used to extract seeds from most of the cones, but manual extraction was required for immature cones with non-reflexed scales. Wings were removed by rubbing seeds in a cotton bag and blowing away debris with a fan; seeds were then individually inspected with a hand lens to remove those with signs of physical damage or seed predation. Germination studies commenced immediately following seed extraction and were conducted according to International Seed Testing Association (ISTA) standards for *P. glauca* (ISTA, 2003). Seeds from each tree were randomly divided into either 4 replicates of 100 seeds (2006) or 8 replicates of at least 10 seeds (2010; the low seed numbers during 2010 resulted from infestation by the spruce seed moth *Cydia strobilella*). Seeds of each replicate were placed on two layers of filter paper (Fisher 09-795A; Fisher Scientific International, Inc., Hampton, New Hampshire) in a covered 60 mm × 15 mm petri dish (Fisher 0875713A; Fisher Scientific International, Inc., Hampton, New Hampshire), and filter papers were saturated with deionized water. To prevent water loss, petri dishes were sealed in $5\frac{3}{4}'' \times 3''$ plastic zipper bags. During 2006, seeds were stratified prior to commencement of germination studies, whereas during 2010 seeds were subjected to "double tests" (ISTA, 2003) in which four of the replicates from each tree were stratified and four were not. Stratification consisted of 21 days storage in a 3–5 °C Conviron E7/2 plant growth chamber (Conviron, Winnipeg, Manitoba) with an 8 h photoperiod at 200 lux (measured using LI-COR LI-185B with quantum sensor LI-190SB; LI-COR Biosciences, Lincoln, Nebraska). Germination studies were conducted during 21 days in the same growth chambers at 25 °C with a 16 h photoperiod at 750 lux. Germination was assessed daily between days 7 and 21. Seeds were considered to have germinated when the radicle was four times longer than the seed (Zasada, 1973; Winston and Haddon, 1981), and germinated seeds were removed daily from each petri dish. Germination rate was plotted as a cumulative function of accumulated degree days, calculated as above using daily temperature data from 2006 (University of Calgary Biogeoscience Institute, Barrier Lake Station) and 2010 (Calgary International Airport; http://climate.weatheroffice.gc.ca). As we were interested in the timing of seed development (and not, for example, in differences between treatments, replicates, trees, or dates), germination rates were calculated by pooling seeds collected on each sampling date.

Germination data were also obtained from the literature for several additional locations (Fig. 2), including Chalk River, Ontario (45°59′00″ N, 77°26′00″ W), Fairbanks, Alaska (64°48′54″ N, 147°51′23″ W), Indian Head, Saskatchewan (50°33′00″ N, 103°39′00″ W), and Kananaskis Country, Alberta (51°01′39″ N, 115°02′05″ W). These data include the "real germination" results of Crossley (1953) and means (±SEM) calculated from trees W-1 and W-2 of Cram and Worden (1957), trees 1–3 from treatment 4 of Zasada (1973), trees 2 and 4–6 from the T-field site of Zasada (1978), and weeks 4, 8, and 12 of the "shack-air" treatment of Winston and Haddon (1981). In these studies, cone sampling began at various times during the spring or summer, but consistently ended upon observation of cone opening. To compare data among locations, sampling dates were expressed in accumulated degree days (as above) using daily temperature data obtained for the appropriate year from weather stations located within 8 km of each sampling site (http://climate.weatheroffice.gc.ca, http://www.ncdc.noaa.gov).

## 4 Results

### 4.1 Simulation of cone heating by crown fire

Simulated fires spread as passive crown fires (Van Wagner, 1977). Crown fuel combustion was dependent on the spreading surface fire, since the product of spread rate and effective bulk density was much less than empirical estimates of the fuel mass flow rate required for crown fire spread (Van Wagner, 1977; Thomas, 1967). For the five simulations, rate of spread was $0.072 \pm 0.004$ (mean $\pm$ SEM) $\mathrm{m\,s^{-1}}$ and fire intensity was $9146.81 \pm 1165.00$ (mean $\pm$ SEM) $\mathrm{kW\,m^{-1}}$. Note that in each simulation, fire spread was not steady-state and that both rate of spread and intensity varied in time and space. Typical simulated time series of cone surface and seed temperatures are shown in Fig. 4. Temperature–time histories at cone surfaces varied widely, but relatively little variation was observed in maximum seed temperatures, which ranged from 46.00 °C to 95.65 °C (Supplement Fig. G1). Variation in maximum seed temperatures varied with time-integrated total heat flux on cone surfaces (Supplement Fig. H1). In general, maximum seed temperatures were greater for cones at 8.7 m than for cones at 17.7 m (Supplement Figs. G1 and H1), which was expected given the greater bulk density (per canopy volume) of crown fuels at 8.7 m and the inverse relation between temperature and height as characterized by classical plume theory (cf. Mercer and Weber, 2001).

Simulation results suggest that white spruce seed contained in closed cones can survive heating by crown fire (Fig. 5). Seed survival is expected for any necrosis temperature greater than 46 °C (a value of 60 °C is generally assumed in fire effects research; Dickinson and Johnson, 2004). For a given seed necrosis temperature, viable seed would be contained in a larger proportion of cones at a height of $z = 17.7$ m than a height of $z = 8.7$ m. Assuming a threshold necrosis temperature of 70 °C for *Picea* seeds (Granström and Schimmel, 1993), viable seed would be contained in approximately 7.5 % of cones at 8.7 m, 19 % of cones at 17.7 m, and 12 % of cones for both heights combined. This should be considered as a conservative estimate given our use of 70 °C for the threshold necrosis temperature (see Sect. 5). The proportion of cones containing viable seed increased with assumed seed necrosis temperature so that all cones at height $z = 17.7$ m would contain viable seed for a necrosis temperature of 81.25 °C, and all cones at height $z = 8.7$ m would contain viable seed for a necrosis temperature of 95.65 °C.

### 4.2 Timing of fire occurrence and seed development

The timing of fire occurrence and seed development at eight locations across the range of white spruce are shown in Fig. 6 (this assumes steady-state rate of spread; the timing of fire occurrence estimated using other assumptions is shown in Supplement Fig. I1). Temporal patterns of seed development

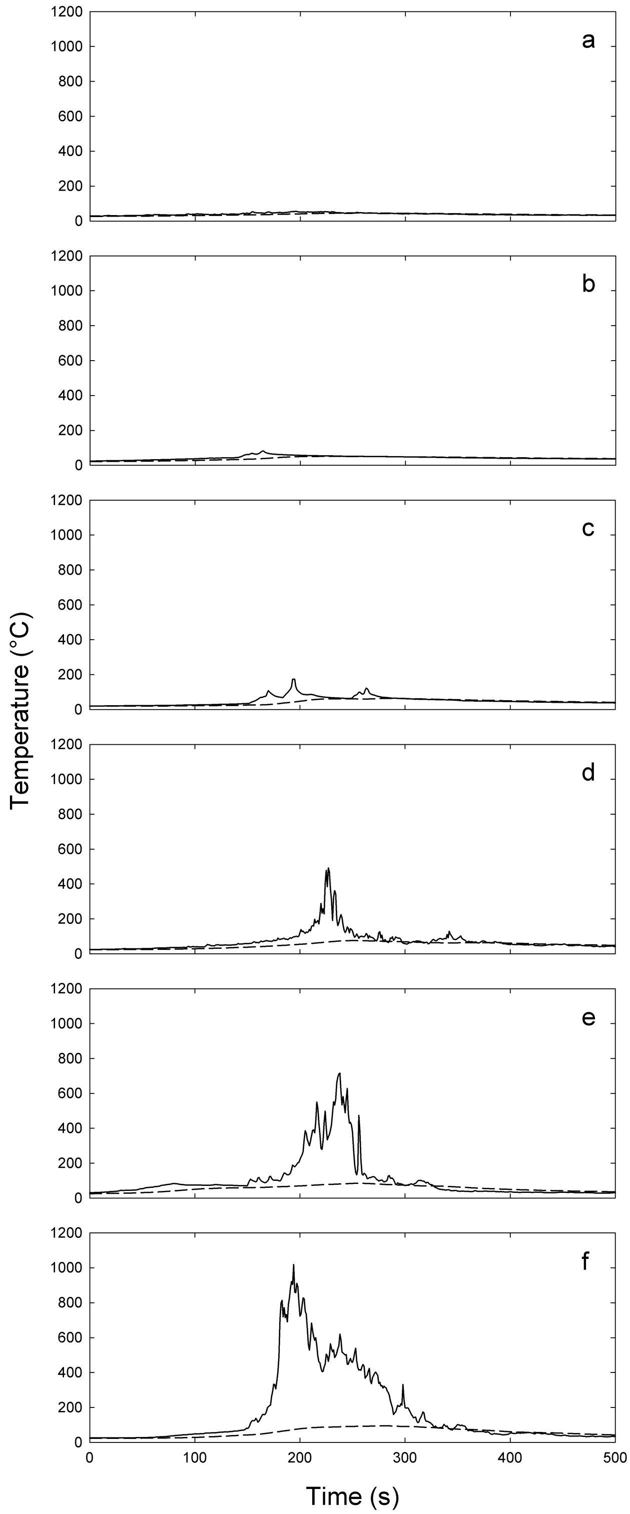


**Fig. 4.** Typical time series of temperatures for cone surfaces ($T_{\mathrm{surf}}$; solid lines) and seeds ($T_{\mathrm{seed}}$; dashed lines). Time series are shown for cones having maximum seed temperatures that span the range of observed values: 46.00 °C **(a)**, 51.17 °C **(b)**, 64.09 °C **(c)**, 75.85 °C **(d)**, 84.62 °C **(e)**, and 93.90 °C **(f)**.

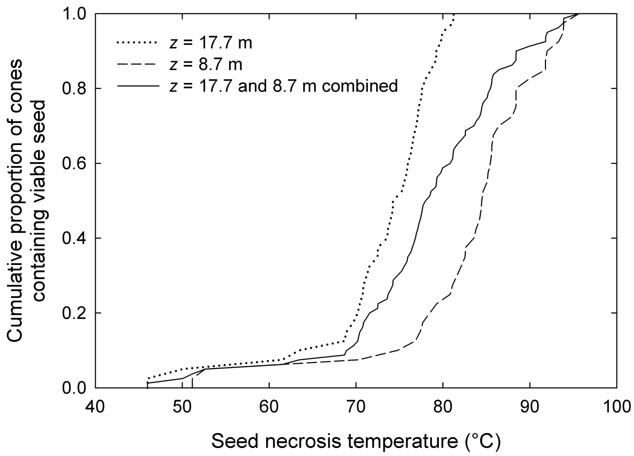


**Fig. 5.** Cumulative proportion of cones containing viable seed as a function of seed necrosis temperature, for cones in five simulated forest fires at heights of $z = 8.7$ m ($N = 40$), $z = 17.7$ m ($N = 40$), and $z = 8.7$ and 17.7 m combined ($N = 80$).

(in accumulated degree days) were highly consistent among locations. The onset of germinability in Calgary occurred at 633.12 degree days for non-stratified seeds and at 705.65 degree days for stratified seeds. Although cone collections at other locations began too late in the year to determine the onset of germinability, extrapolation of results suggests that roughly 600 degree days are required for seed germinability. In general, germination rates increased sigmoidally and saturated prior to cone opening (Fig. 6). Accumulated degree days required for cone opening varied among locations, with a mean of 1177.29 (±71.38 SEM) degree days. Differences in date of cone opening may result from local differences in growing season length (i.e., total accumulated degree days per year) or differences in how investigators perceived cone opening.

The proportion of total area burned resulting from fires that occur when seeds are germinable but still contained within closed cones can be estimated for each area as the difference between area burned after 600 degree days (onset of cone opening) and area burned after 1177 degree days (cone opening; Fig. 6). This proportion varies from 0.14 at Schefferville to 0.90 at Jasper, with a mean of 0.52 (±0.091 SEM). Thus, across the range of white spruce, approximately half of the total area burned resulted from fires that occurred when seeds would be sufficiently developed to germinate but still insulated within closed cones.

## 5 Discussion

In this paper, white spruce was used to demonstrate that the availability of non-serotinous aerial seed banks after fire is governed by the insulating ability of cone-bearing structures and the relative timing of fire and seed development. Numerical simulations of cone heating in crown fires predicted that approximately 12 % of cones would contain viable seed following the fire, assuming a threshold necrosis temperature of 70 °C (Fig. 5). Fire occurrence and seed germination data suggested that approximately half of the of the area burned within eight fire observation areas (Fig. 2) resulted from fires that occurred when germinable seed would be contained within closed cones during a mast year (Fig. 6). Together, these results are consistent with the hypothesis that white spruce may colonize burned areas from in situ aerial seed banks, provided the fire occurs when germinable seed is contained within closed cones. This is probably rare, however, as it depends on the joint probability (perhaps 0.05) of a mid- to late-season fire (i.e., a fire when germinable seed is still contained in closed cones; mean probability of 0.52) coinciding with a mass-seeding event (probability of 0.1, depending on how masting is defined; Greene and Johnson, 2004). This may explain why the density of white spruce is typically highest along old burn edges and lower across the rest of the landscape (as if recolonization had relied upon long distance dispersal from burn edges; Galipeau et al., 1997; Greene and Johnson, 2000; Peters et al., 2005), but can sometimes be very high (approaching a monoculture) in areas far from old burn edges.

Two assumptions in our reasoning need to be justified. First, we assume that the period when seeds can survive fire ends with the onset of ovulate scale opening. Seed abscission in this species is a slow process, with the 50th percentile of abscission occurring at least a month after the onset of cone opening (Greene et al., 1999). However, this is probably unimportant because relatively small proportions of the total area burned result from fires occurring after cone opening (Fig. 6). Furthermore, once their scales begin to reflex open (a result of differential hygroscopic expansion of sclerid and fiber cells; Dawson et al., 1997), cones will combust like fine fuels (Almeida et al., 2011; Fonda and Varner, 2004) and any seeds they contain will be killed.

Second, our simulations considered the heating of isolated cones, but the majority of white spruce cones (or the seed-bearing structures of any masting species) develop during mass-seeding events (Greene and Johnson, 2004) and are thus not isolated, but instead located within dense clusters of up to several hundred cones. This clustering should provide even greater resistance to heat transfer than is considered in the present simulations (Judd and Ashton, 1991), with a resultant increase in the proportion of cones containing viable seed after the fire. A case in point is black spruce, a serotinous species for which cones characteristically accumulate in a large cluster at the top of the crown. Approximately 50 % of black spruce seeds survive stand-replacing crown fires (Greene and Johnson, 1999; D. F. Greene, unpublished data), a much higher survival rate than predicted for the isolated cones in our simulations. Given the similarity of scale thickness (seed depth) and diameter of white and black spruce cones (Parker and McLachlan, 1978), this difference

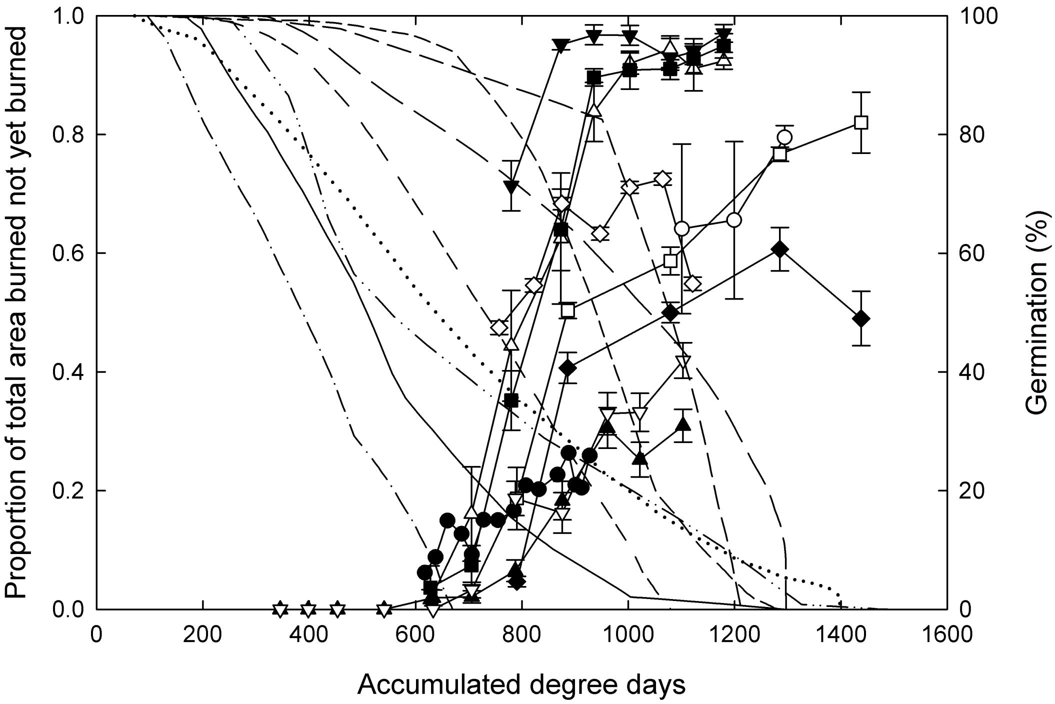


**Fig. 6.** Timing of fire occurrence (descending lines) and white spruce seed development (mean and SEM). Fire occurrence data were estimated assuming steady-state rate of spread between fire start and end dates. Error bars are standard error. ▲ Calgary, non-stratified (2010 data); ▽ Calgary, stratified (2010 data); ⧫ Chalk River, non-stratified (Winston and Haddon, 1981); □ Chalk River, stratified (Winston and Haddon, 1981); ■ Fairbanks, non-stratified (Zasada, 1978); ▼ Fairbanks, stratified (Zasada, 1973); △ Fairbanks, stratified (Zasada, 1978); ○ Indian Head, stratified (Cram and Worden, 1957); • Kananaskis Country (Crossley, 1953); ◊ Kananaskis Country, stratified (2006 data); ——— Bagotville; — — — Fairbanks; – – – Fort Smith; - - - - - - - Jasper; · · · · · · · · · La Ronge; – · – · – · – Schefferville; – · · – · · – · – Sioux Lookout; -- -- -- Yellowknife.

probably reflects the insulating properties of the cluster and not just that of the individual cones. This does not, however, change our conclusion that the joint probability of mid- to late-season fires and mass-seeding events makes in situ white spruce recruitment rare; instead, it simply means that the density of regeneration during these rare events would be higher than our simulation results suggest.

Maximum seed temperatures varied with time-integrated total heat flux on cone surfaces (Supplement Fig. H1). Because integrated heat fluxes result from convective and radiative heat transfer from the flame and plume to cone surfaces, it is desirable to relate this integrated flux to some measure of heat output from the fire. The most widely used measure is fire intensity (Byram, 1959), which was initially developed as a time- and space-averaged approximation of heat output for use in management and suppression of fires (Van Wagner, 1965). However, intensity can vary spatially and temporally within fires due to changes in wind velocity and fuel bulk density (Fig. 3; Byram, 1959; Van Wagner, 1965). Further, the relationships between intensity and heat flux incident on cone surfaces also vary in accordance with flame geometry, cone locations, and patterns of air and plume flow. Consequently, it is difficult to identify relevant fire intensities and their contributions to cone surface heat fluxes. While it is possible to obtain reasonable statistical relationships between time-integrated heat flux and cone heating time, height, and fire intensity (Supplement J), it is still not clear how or why these variables contribute to the heat fluxes incident on cone surfaces. A more insightful approach might be to identify the areas of the forest from which the incident fluxes could have originated. Methods similar to those used for flux footprint modeling (Schmid, 2002; Vesala et al., 2008) seem particularly suited for use with the CFD approach, as CFD models already compute the paths of convective and radiative heat transfer from the fire to the cone surfaces.

The proportion of cones containing viable seed following crown fire was estimated by comparing variation in maximum seed temperatures (Supplement Fig. H1) to an assumed threshold necrosis temperature (Fig. 5). This approach was used in lieu of a more mechanistic rate-process approach (Dickinson and Johnson, 2004; Dickinson et al., 2004), because cellular necrosis kinetics have not been established for white spruce seeds. The threshold necrosis temperature of 70 °C (Granström and Schimmel, 1993) assumed in this study should be considered a conservative estimate, as it was measured using a heat exposure time of 10 min, which is much longer than the exposure time of seeds in our simulations (maximum of approximately 3 min; Fig. 4). Given this relatively short exposure time, and the exponential increase of cell necrosis rates with temperature (Dickinson and Johnson, 2004; Johnson et al., 1974), a necrosis temperature greater than 70 °C is expected for seeds in cones. Consequently, the proportion of cones containing viable seed (12 %; Fig. 5) is also expected to be greater following crown fires. Nevertheless, during a mass-seeding event, even this small proportion of cones would contribute an enormous number of seeds for post-fire recruitment. For example, assuming a viable seed density of 2600 seeds $m^{-2}$ (a mast crop in Alaska; Zasada, 1985), this 12 % survival rate would yield 312 seeds $m^{-2}$. Approximately 5 % of these seeds would become seedlings after three years given typical granivory rates and proportions of suitable seedbeds created by smoldering combustion (Charron and Greene, 2002), for a total of approximately 15 seedlings $m^{-2}$.

The onset of germinability is remarkably consistent across the range of white spruce (Fig. 6). Even better agreement might be obtained if degree day calculations were started on pollination dates (Zasada, 1973; Edwards, 1980) instead of ordinal day 1, but unfortunately these data were not available for any of the locations considered in this study. Nevertheless, if these patterns hold across the range of white spruce, the onset of germinability at Schefferville (approximately 240 km south of the arctic tree line; Vowinckel et al., 1975) would not occur until early September, because degree days accumulate more slowly at higher latitudes. This would support previous conclusions (Black and Bliss, 1980) that tree line represents a climate regime where degree day accumulation over the growing season is insufficient for seed maturation. Thus, tree line may be maintained or expanded during uncharacteristically warm summers (when 600 degree days are reached unusually early) that coincide with a mast year. These results should also contribute to the development of detailed models of woody plant migration rates in response to climate change.

Despite consistency in the onset of germinability, the timing of cone opening appeared to vary over the range of white spruce (Fig. 6). It is unclear whether these differences result from differences in how investigators perceived cone opening, or whether phenological differences actually do exist. Because the retention of germinable seed in closed, insulative cones is adaptive in boreal fire regimes, one might expect seed release to be timed with the end of the fire season. For example, earlier dates of seed release may be expected at Bagotville and Yellowknife, whereas later release dates may be expected at La Ronge and Sioux Lookout. Future work should consider how variation in regional fire seasons controls variation in regional seed release dates, and also develop a protocol for assessing cone opening in local populations with a view to their changing combustibility.

Variation in germination rates among locations (Fig. 6) probably reflects differences in calculation of germination rate among studies. For example, the highest reported values (Zasada, 1978, 1973) were "real germination" rates for which unfilled seeds were excluded from calculations, whereas the lowest reported rates (Crossley, 1953; our 2010 samples) were "apparent germination" rates for which unfilled seeds were included. Additionally, the relatively low germination rates observed in our 2010 samples reflect an outbreak of the spruce seed moth (*C. strobilella*) and their preferential selection of filled seeds (Tripp and Hedlin, 1956).

In this study, the WFDS fire behavior model was used as a physics-based "laboratory" for conducting virtual experiments on forest fire spread, cone heating, and seed necrosis. This approach has several advantages that make it a valuable complement to empirical field studies. For example, simulated fire experiments are safe, relatively fast, not limited to the fire season, and easily rerun to accommodate desired changes. They are also useful for addressing questions that are difficult or impossible to study in the field, such as seed survival for non-serotinous masting species (as in this study, for example). The approach is also advantageous because it considers the causal mechanisms linking combustion, fluid dynamics, and heat transfer to the biophysics and physiology or organisms and their consequent effects at higher levels of organization such as forest stands and ecosystems. Consequently, the relevant variables and their functional relationships are clearly defined, and sensitivity analyses can be used to identify the most important variables in a particular scenario (Supplement A and C). The use of CFD modeling has been growing in the fire behavior literature (e.g., Mell et al., 2007; Dupuy et al., 2011; Linn et al., 2010; Morvan et al., 2011; Hoffmann et al., 2012; Mell et al., 2009), but we are aware of only one paper that has applied the approach to questions of fire ecology (Bova et al., 2011). It is hoped that this approach will become more common and help to foster a more mechanistic and predictive fire ecology.

It is important to note that while WFDS directly simulates (to some approximation) all of the recognized, coupled, physical processes that govern fire behavior, the model has not been validated for the specific crown fire scenarios simulated in this paper. Validation and verification tests have been conducted for isolated (e.g., radiant heat transfer from a known hot object to a target) and coupled (e.g., buoyancy-induced plume rise due to combustion in a pool fire; fire spread through a Douglas fir tree) component physical processes (McDermott et al., 2010; McGrattan et al., 2010b; Mell et al., 2009). However, no measurements have been obtained for the convective and radiant heat fluxes within tree crowns during passive crown fires of the type considered in this study. For this reason, we emphasize that this study is exploratory in nature, and is an example of the state of process-based fire behavior modeling and its use as a predictive tool. In the future, properly designed field and laboratory measurements will provide validation datasets for these types of fire behavior models. However, it will not be possible to measure all the relevant scenarios. Thus, when used carefully, these types of models offer one way of exploring physical processes and testing hypotheses for large fires and complex fuels.

We have proposed that the retention of germinable seed in closed, insulative cones is a fire-adaptive trait (Keeley et al., 2011) that enables non-serotinous species to exist in fire regimes that should theoretically favor serotiny (Enright et al., 1998; Lamont and Enright, 2000). This contrasts with the common assumption that non-serotinous seed-bearing structures have little to no fire-adaptive value (Fonda and Varner, 2004). However, the success of this colonization strategy relies on the coincidence of a mast year and a fire that occurs when germinable seed is contained in closed cones. Consequently, serotiny provides a greater advantage, as it helps ensure that seeds are consistently available regardless of the timings fire or seed development.

**Supplementary material related to this article is available online at: http://www.biogeosciences.net/10/5061/2013/bg-10-5061-2013-supplement.pdf.**

*Acknowledgements.* The authors thank D. S. Phillips for high-performance computing assistance, K. B. McGrattan for FDS modeling advice, R. Poitras for assistance in preparing Fig. 2, J. Swann for identification of *C. strobilella*, and an anonymous referee for constructive comments during the review process. This research was enabled by the use of computing resources provided by WestGrid and Compute/Calcul Canada, and was supported by Alberta Ingenuity, NSERC-Discovery, GEOIDE (GEOmatics for Informed Decisions), and the International Association of Wildland Fire.

Edited by: P. Stoy

## References

Albini, F. A.: Estimating Wildfire Behavior and Effects, USDA Forest Service General Technical Report INT-30, 1976.

Albini, F. A. and Baughman, R. G.: Estimating Windspeeds for Predicting Wildland Fire Behavior, USDA Forest Service Reserach Paper INT-221, 1979.

Alexander, M. E., Stocks, B. J., and Lawson, B. D.: Fire Behavior in Black Spruce-Lichen Woodland: The Porter Lake Project, Forestry Canada Information Report NOR-X-310, 1991.

Allen, J. C.: A modified sine wave method for calculating degree days, Environ. Entomol., 5, 388–396, 1976.

Almeida, M., Viegas, D. X., Miranda, A. I., and Reva, V.: Effect of particle orientation and of flow velocity on the combustibility of Pinus pinaster and Eucalyptus globulus firebrand material, Int. J. Wildland Fire, 20, 946–962, doi:10.1071/WF09080, 2011.

Beaufait, W. R.: Some effects of high temperatures on the cones and seeds of jack pine, Forest Sci., 6, 194–199, 1960.

Black, R. A. and Bliss, L. C.: Reproductive ecology of Picea mariana (Mill.) BSP., at tree line near Inuvik, Northwest Territories, Canada, Ecol. Monogr., 50, 331–354, 1980.

Boggs, K., Sturdy, M., Rinella, D. J., and Rinella, M. J.: White spruce regeneration following a major spruce beetle outbreak in forests on the Kenai Peninsula, Alaska, Forest Ecol. Manag., 255, 3571–3579, doi:10.1016/j.foreco.2008.02.039, 2008.

Bova, A. S., Bohrer, G., and Dickinson, M. B.: A model of gas mixing into single-entrance tree cavities during wildland fires, Can. J. Forest Res., 41, 1659–1670, doi:10.1139/x11-077, 2011.

Bradstock, R. A., Gill, A. M., Hastings, S. M., and Moore, P. H. R.: Survival of serotinous seedbanks during bushfires: Comparative studies of Hakea species from southeastern Australia, Aust. J. Ecol., 19, 276–282, doi:10.1111/j.1442-9993.1994.tb00490.x, 1994.

Brown, J. K.: Weight and Density of Crowns of Rocky Mountain Conifers, USDA Forest Service Research Paper INT-197, 1978.

Byram, G. M.: Combustion of Forest Fuels, in: Forest Fire: Control and Use, edited by: Davis, K. P., McGraw-Hill Book Company, Inc., New York, 1959.

Chapra, S. C. and Canale, R. P.: Numerical Methods for Engineers, Sixth Edn., McGraw-Hill, New York, 2009.

Charron, I. and Greene, D. F.: Post-wildfire seedbeds and tree establishment in the southern mixedwood boreal forest, Can. J. Forest Res., 32, 1607–1615, doi:10.1139/x02-085, 2002.

Chrosciewicz, Z.: Foliar moisture content variations in four coniferous tree species of central Alberta, Can. J. Forest Res., 16, 157–162, doi:10.1139/x86-029, 1986.

Cram, W. H. and Worden, H. A.: Maturity of white spruce cones and seed, Forest Sci., 3, 263–269, 1957.

Crossley, D. I.: Seed maturity in white spruce, Silviculture Research Notes No. 104, Canada Department of Resources and Development, Forestry Branch, 1953.

Dawson, C., Vincent, J. F. V., and Rocca, A.-M.: How pine cones open, Nature, 390, 668–668, 1997.

Despain, D., Clark, D., and Reardon, J.: Simulation of crown fire effects on canopy seed bank in lodgepole pine, Int. J. Wildland Fire, 6, 45–49, doi:10.1071/WF9960045, 1996.

Dickinson, M. B. and Johnson, E. A.: Temperature-dependent rate models of vascular cambium cell mortality, Can. J. Forest Res., 34, 546–559, doi:10.1139/x03-223, 2004.

Dickinson, M. B., Jolliff, J., and Bova, A. S.: Vascular cambium necrosis in forest fires: using hyperbolic temperature regimes to estimate parameters of a tissue-response model, Aust. J. Bot., 52, 757–763, doi:10.1071/BT03111, 2004.

Dupuy, J.-L., Linn, R. R., Konovalov, V., Pimont, F., Vega, J. A., and Jiménez, E.: Exploring three-dimensional coupled fire–atmosphere interactions downwind of wind-driven surface fires and their influence on backfires using the HIGRAD-FIRETEC model, Int. J. Wildland Fire, 20, 734–750, doi:10.1071/WF10035, 2011.

Edwards, D. G. W.: Maturity and quality of tree seeds – a state-of-the-art review, Seed Sci. Technol., 8, 625–657, 1980.

Enright, N. J., Marsula, R., Byron, B. L., and Wissel, C.: The ecological significance of canopy seed storage in fire-prone environments: A model for non-sprouting shrubs, J. Ecol., 86, 946–959, 1998.

Fonda, R. W. and Varner, J. M.: Burning characteristics of cones from eight pine species, Northwest Sci., 78, 322–333, 2004.

Fraver, S.: The insulating value of serotinous cones in protecting pitch pine (*Pinus rigida*) seeds from high temperatures, J. Pennsylvania Acad. Sci., 65, 112–116, 1992.

Galipeau, C., Kneeshaw, D. D., and Bergeron, Y.: White spruce and balsam fir colonization of a site in the southeastern boreal forest as observed 68 years after fire, Can. J. Forest Res., 27, 139–147, doi:10.1139/x96-148, 1997.

Gauthier, S., Bergeron, Y., and Simon, J.-P.: Effects of fire regime on the serotiny level of jack pine, J. Ecol., 84, 539–548, 1996.

Giedt, W. H.: Investigation of variation of point unit heat-transfer coefficient around a cylinder normal to an air stream, T. Am. Soc. Mech. Eng., 71, 375-381, 1949.

Gill, A. M.: Adaptive responses of Australian vascular plant species to fires, in: Fire and the Australian biota, edited by: Gill, A. M., Groves, R. H., and Noble, I. R., Australian Academy of Science, Canberra, 1981.

Granström, A. and Schimmel, J.: Heat effects on seeds and rhizomes of a selection of boreal forest plants and potential reaction to fire, Oecologia, 94, 307–313, doi:10.1007/bf00317103, 1993.

Greene, D. F. and Johnson, E. A.: Modelling recruitment of Populus tremuloides, Pinus banksiana, and Picea mariana following fire in the mixedwood boreal forest, Can. J. Forest Res., 29, 462–473, doi:10.1139/x98-211, 1999.

Greene, D. F. and Johnson, E. A.: Tree recruitment from burn edges, Can. J. Forest Res., 30, 1264–1274, doi:10.1139/x00-040, 2000.

Greene, D. F. and Johnson, E. A.: Modelling the temporal variation in the seed production of North American trees, Can. J. Forest Res., 34, 65–75, doi:10.1139/x03-188, 2004.

Greene, D. F., Zasada, J. C., Sirois, L., Kneeshaw, D., Morin, H., Charron, I., and Simard, M. J.: A review of the regeneration dynamics of North American boreal forest tree species, Can. J. Forest Res., 29, 824–839, doi:10.1139/x98-112, 1999.

Greene, D. F., Messier, C., Asselin, H., and Fortin, M.-J.: The effect of light availability and basal area on cone production in Abies balsamea and Picea glauca, Can. J. Bot., 80, 370–377, doi:10.1139/b02-020, 2002.

Grønli, M. G., Várhegyi, G., and Di Blasi, C.: Thermogravimetric analysis and devolatilization kinetics of wood, Ind. Eng. Chem. Res., 41, 4201–4208, doi:10.1021/ie0201157, 2002.

Gupta, M., Yang, J., and Roy, C.: Specific heat and thermal conductivity of softwood bark and softwood char particles, Fuel, 82, 919–927, doi:10.1016/s0016-2361(02)00398-8, 2003.

Gutsell, S. L. and Johnson, E. A.: Accurately ageing trees and examining their height-growth rates: Implications for interpreting forest dynamics, J. Ecol., 90, 153–166, 2002.

Hoffmann, C. M., Morgan, P., Mell, W. E., Parsons, R. A., Strand, E. K., and Cook, S.: Numerical simulation of crown fire hazard immediately following bark beetle-caused tree mortality in lodgepole pine forests, Forest Sci., 58, 178–188, 2012.

Holman, J. P.: Heat Transfer, 8th Edn., McGraw-Hill Inc., New York., 1997.

Incropera, F. P., De Witt, D. P., Bergman, T. L., and Lavine, A. S.: Fundamentals of heat and mass transfer, 6th Edn., John Wiley and Sons Inc., New York, NY, 1024 pp., 2006.

ISTA: International Rules for Seed Testing, Edition 2003, The International Seed Testing Association, Basserdorf, 2003.

Johnson, A. F., Woodard, P. M., and Titus, S. J.: Lodgepole pine and white spruce crown fuel weights predicted from diameter at breast height, Forest. Chron., 66, 596–599, 1990.

Johnson, E. A.: Fire and Vegetation Dynamics: Studies from the North American Boreal Forest, Cambridge University Press, Cambridge, 1992.

Johnson, E. A. and Fryer, G. I.: Why Engelmann spruce does not have a persistent seed bank, Can. J. Forest Res., 26, 872–878, doi:10.1139/x26-095, 1996.

Johnson, E. A., Miyanishi, K., and Kleb, H.: The hazards of interpretation of static age structures as shown by stand reconstructions in a *Pinus contorta – Picea engelmannii* forest, J. Ecol., 82, 923–931, 1994.

Johnson, E. A., Morin, H., Miyanishi, K., Gagnon, R., and Greene, D. F.: A process approach to understanding disturbance and forest dynamics for sustainable forestry, in: Towards Sustainable Management in the Boreal Forest, edited by: Burton, P. J., Messier, C., Smith, D. W., and Adamowicz, W. L., NRC Research Press, Ottawa, 2003.

Johnson, F. H., Eyring, H., and Stover, B. J.: The theory of rate processes in biology and medicine, John Wiley & Sons, New York, 1974.

Judd, T. and Ashton, D.: Fruit clustering in the Myrtaceae: Seed survival in capsules subjected to experimental heating, Aust. J. Bot., 39, 241–245, doi:10.1071/BT9910241, 1991.

Judd, T. S.: Seed survival in small myrtaceous capsules subjected to experimental heating, Oecologia, 93, 576–581, doi:10.1007/bf00328968, 1993.

Keane, R. E. and Dickinson, L. J.: Development and Evaluation of the Photoload Sampling Technique, USDA Forest Service Research Paper RMRS-RP-61CD, 2007.

Keeley, J. E., Pausas, J. G., Rundel, P. W., Bond, W. J., and Bradstock, R. A.: Fire as an evolutionary pressure shaping plant traits, Trends Plant Sci., 16, 406–411, doi:10.1016/j.tplants.2011.04.002, 2011.

Kiil, A. D.: Fire spread in a black spruce stand, Canadian Forest Service Bi-Monthly Research Notes, 31, 2–3, 1975.

Koike, T.: Leaf structure and photosynthetic performance as related to the forest succession of deciduous broad-leaved trees, Plant Spec. Biol., 3, 77–87, doi:10.1111/j.1442-1984.1988.tb00173.x, 1988.

Lamont, B., Le Maitre, D., Cowling, R., and Enright, N.: Canopy seed storage in woody plants, Bot. Rev., 57, 277–317, doi:10.1007/bf02858770, 1991.

Lamont, B. B. and Enright, N. J.: Adaptive advantages of aerial seed banks, Plant Spec. Biol., 15, 157–166, doi:10.1046/j.1442-1984.2000.00036.x, 2000.

Lawson, B. D. and Armitage, O. B.: Weather Guide for the Canadian Forest Fire Danger Rating System, Natural Resources Canada, 2008.

Le Maitre, D. C.: Current interpretations of the term serotiny, S. Afr. J. Sci., 81, 289–290, 1985.

Linn, R., Reisner, J., Colman, J. J., and Winterkamp, J.: Studying wildfire behavior using FIRETEC, Int. J. Wildland Fire, 11, 233–246, doi:10.1071/WF02007, 2002.

Linn, R. R., Winterkamp, J. L., Weise, D. R., and Edminster, C.: A numerical study of slope and fuel structure effects on coupled wildfire behaviour, Int. J. Wildland Fire, 19, 179–201, doi:10.1071/WF07120, 2010.

Little, E. L.: Atlas of United States trees. Volume 1. Conifers and important hardwoods, US Department of Agriculture Miscellaneous Publication 1146, 1971.

Lutz, H. J.: Ecological Effects of Forest Fires in the Interior of Alaska, US Department of Agriculture Technical Bulletin 1133, 1956.

Macias Fauria, M. and Johnson, E. A.: Large-scale climatic patterns control large lightning fire occurrence in Canada and Alaska forest regions, J. Geophys. Res., 111, G04008, doi:10.1029/2006jg000181, 2006.

Macias Fauria, M., Michaletz, S. T., and Johnson, E. A.: Predicting climate change effects on wildfires requires linking processes across scales, Wiley Interdisciplinary Reviews: Climate Change, 2, 99–112, doi:10.1002/wcc.92, 2011.

McDermott, R., McGrattan, K., Hostikka, S., and Floyd, J.: Fire Dynamics Simulator (Version 5) Technical Reference Guide Volume 2: Verification, NIST Special Publications 1018-5, 2010.

McGrattan, K.: Cable Response to Live Fire (CAROLFIRE) Volume 3: Cable Fire Response Data for Fire Model Improvement, NUREG/CR-6931V2, NISTIR 7472, US Nuclear Regulatory Commission, 2008.

McGrattan, K., Hostikka, S., Floyd, J., Baum, H. R., Rehm, R. G., Mell, W. E., and McDermott, R.: Fire Dynamics Simulator (Version 5) Technical Reference Guide Volume 1: Mathematical Model, NIST Special Publications 1018-5, 2010a.

McGrattan, K., Hostikka, S., Floyd, J., and McDermott, R.: Fire Dynamics Simulator (Version 5) Technical Reference Guide Volume 3: Validation, NIST Special Publication 1018-5, 2010b.

Mell, W., Maranghides, A., McDermott, R., and Manzello, S. L.: Numerical simulation and experiments of burning douglas fir trees, Combust. Flame, 156, 2023–2041, doi:10.1016/j.combustflame.2009.06.015, 2009.

Mell, W. M., Jenkins, M. A., Gould, J., and Cheney, P.: A physics-based approach to modelling grassland fires, Int. J. Wildland Fire, 16, 1–22, doi:10.1071/WF06002, 2007.

Mercer, G., Gill, A., and Weber, R.: A time-dependent model of fire impact on seed survival in woody fruits, Aust. J. Bot., 42, 71–81, doi:10.1071/BT9940071, 1994.

Mercer, G. N. and Weber, R. O.: Fire Plumes, in: Forest Fires: Behavior and Ecological Effects, edited by: Johnson, E. A. and Miyanishi, K., Academic Press, New York, 2001.

Michaletz, S. T. and Johnson, E. A.: A heat transfer model of crown scorch in forest fires, Can. J. Forest Res., 36, 2839–2851, doi:10.1139/x06-158, 2006.

Miyanishi, K.: Duff consumption, in: Forest Fires: Behavior and Ecological Effects, edited by: Johnson, E. A. and Miyanishi, K., Academic Press, New York, 2001.

Monteith, J. L. and Unsworth, M. H.: Principles of Environmental Physics. Third Edition., Academic Press, New York, 2008.

Morvan, D. and Dupuy, J. L.: Modeling of fire spread through a forest fuel bed using a multiphase formulation, Combust. Flame, 127, 1981–1994, doi:10.1016/s0010-2180(01)00302-9, 2001.

Morvan, D. and Dupuy, J. L.: Modeling the propagation of a wildfire through a Mediterranean shrub using a multiphase formulation, Combust. Flame, 138, 199–210, doi:10.1016/j.combustflame.2004.05.001, 2004.

Morvan, D., Hoffman, C., Rego, F., and Mell, W.: Numerical simulation of the interaction between two fire fronts in grassland and shrubland, Fire Safety J., 46, 469–479, doi:10.1016/j.firesaf.2011.07.008, 2011.

Nienstadt, H. and Zasada, J. C.: Picea glauca (Moench) Voss. White spruce, in: Silvics of North America, Volume 1. Conifers, edited by: Burns, R. M. and Honkala, B. H., US Dept of Agriculture Handbook No. 654, 204–226, 1990.

Norum, R. A.: Predicting Wildfire Behavios in Black Spruce Forests in Alaska, USDA Forest Service Research Note PNW-401, 1982.

Norum, R. A.: Wind Adjustment Factors for Predicting Fire Behavior in Three Fuel Types in Alaska, USDA Forest Service Research Paper PNW-309, 1983.

O'Donnell, J. A., Romanovsky, V. E., Harden, J. W., and McGuire, A. D.: The effect of moisture content on the thermal conductivity of moss and organic soil horizons from black spruce ecosystems in interior Alaska, Soil Sci., 174, 646–651, 2009.

Ottmar, R. D. and Vihnanek, R. E.: Stereo photo series for quantifying natural fuels, Volume II: Black spruce and white spruce types in Alaska, PMS. 831, National Wildfire Coordinating Group, National Interagency Fire Center, Boise, ID, 1998.

Ottmar, R. D., Sandberg, D. V., Riccardi, C. L., and Prichard, S. J.: An overview of the Fuel Characteristic Classification System – Quantifying, classifying, and creating fuelbeds for resource planning, Can. J. Forest Res., 37, 2383–2393, doi:10.1139/x07-077, 2007.

Parker, W. H. and McLachlan, D. G.: Morphological variation in white and black spruce: investigation of natural hybridization between Picea glauca and P. mariana, Can. J. Bot., 56, 2512–2520, doi:10.1139/b78-303, 1978.

Parsons, R. A., Mell, W. E., and McCauley, P.: Linking 3D spatial models of fuels and fire: Effects of spatial heterogeneity on fire behavior, Ecol. Model., 222, 679–691, doi:10.1016/j.ecolmodel.2010.10.023, 2011.

Payette, S.: Fire as a controlling process in the North American boreal forest, in: A Systems Analysis of the Global Boreal Forest, edited by: Shugart, H. H., Leemans, R., and Bonan, G. B., Cambridge University Press, Cambridge, 1992.

Peters, V. S., Macdonald, S. E., and Dale, M. R. T.: The interaction between masting and fire is key to white spruce regeneration, Ecology, 86, 1744–1750, doi:10.1890/03-0656, 2005.

Ragland, K. W., Aerts, D. J., and Baker, A. J.: Properties of wood for combustion analysis, Bioresource Technol., 37, 161–168, doi:10.1016/0960-8524(91)90205-x, 1991.

Rehm, R. G. and Baum, H. R.: The equations of motion for thermally driven, buoyant flows, J. Res. Nat. Bur. Stand., 83, 297–308, 1978.

Rolf, T. and Adrian, B.: spatstat: An R package for analyzing spatial point patterns, J. Stat. Softw., 12, 1–42, 2005.

Rothermel, R. C.: A mathematical model for predicting fire spread in wildland fuels, USDA Forest Service Reserach Paper INT-115, Ogden, UT, 1972.

Rothermel, R. C.: Predicting Behavior and Size of Crown Fires in the Northern Rocky Mountains, USDA Forest Service Reserach Paper INT-438, Ogden, 1991.

Schmid, H. P.: Footprint modeling for vegetation atmosphere exchange studies: a review and perspective, Agr. Forest Meteorol., 113, 159–183, doi:10.1016/s0168-1923(02)00107-7, 2002.

Schwilk, D. W. and Ackerly, D. D.: Flammability and serotiny as strategies: correlated evolution in pines, Oikos, 94, 326–336, doi:10.1034/j.1600-0706.2001.940213.x, 2001.

Simpson, W. and TenWolde, A.: Wood Handbook: Wood as an Engineering Material, USDA Forest Service General Technical Report FPL-GTR-113, Madison, 1999.

Singh, T.: Wood density variations in thirteen Canadian tree species, Wood Fiber Sci., 19, 362–369, 1987.

Stocks, B. J., Mason, J. A., Todd, J. B., Bosch, E. M., Wotton, B. M., Amiro, B. D., Flannigan, M. D., Hirsch, K. G., Logan, K. A., Martell, D. L., and Skinner, W. R.: Large forest fires in Canada, 1959–1997, J. Geophys. Res., 107, 8149, doi:10.1029/2001jd000484, 2002.

Susott, R. A.: Differential scanning calorimetry of forest fuels, Forest Sci., 28, 839–851, 1982a.

Susott, R. A.: Characterization of the thermal properties of forest fuels by combustible gas analysis, Forest Sci., 28, 404–420, 1982b.

Sylvester, T. W. and Wein, R. W.: Fuel characteristics of arctic plant species and simulated plant community flammability by Rothermel's model, Can. J. Bot., 59, 898–907, doi:10.1139/b81-125, 1981.

Thomas, P. H.: Some aspects of the growth and spread of fire in the open, Forestry, 40, 139–164, doi:10.1093/forestry/40.2.139, 1967.

Thompson, K. and Grime, J. P.: Seasonal variation in the seed banks of herbaceous species in ten contrasting habitats, J. Ecol., 67, 893–921, 1979.

Titus, S., Woodard, P., and Johnson, A.: Sampling intensity for estimating fuel moisture content in lodgepole pine and white spruce trees, Int. J. Wildland Fire, 2, 1–6, doi:10.1071/WF9920001, 1992.

Tripp, H. A. and Hedlin, A. F.: An ecological study and damage appraisal of white spruce cone insects, Forest. Chron., 32, 400–410, 1956.

Van Wagner, C. E.: Describing forest fires – Old ways and new, Forest. Chron., 41, 301–305, 1965.

Van Wagner, C. E.: Conditions for the start and spread of crown fire, Can. J. Forest Res., 7, 23–34, doi:10.1139/x77-004, 1977.

Vesala, T., Kljun, N., Rannik, Ü., Rinne, J., Sogachev, A., Markkanen, T., Sabelfeld, K., Foken, T., and Leclerc, M. Y.: Flux and concentration footprint modelling: State of the art, Environ. Pollut., 152, 653–666, doi:10.1016/j.envpol.2007.06.070, 2008.

Viereck, L. A., Dyrness, C. T., Batten, A. R., and Wenzlick, K. J.: The Alaska Vegetation Classification, US Forest Service General Technical Report PNW-GTR-286, Portland, OR, 1992.

Vowinckel, T., Oechel, W. C., and Boll, W. G.: The effect of climate on the photosynthesis of Picea mariana at the subarctic tree line. 1. Field measurements, Can. J. Bot., 53, 604–620, doi:10.1139/b75-076, 1975.

Wilson, R.: Reformulation of Forest Fire Spread Equations in SI Units, USDA Forest Service Research Note INT-292, 1980.

Winston, D. A. and Haddon, B. D.: Effects of early cone collection and artificial ripening on white spruce and red pine germination, Can. J. Forest Res., 11, 817–826, doi:10.1139/x81-117, 1981.

Wirth, C., Lichstein, J. W., Dushoff, J., Chen, A., and Chapin, F. S.: White spruce meets black spruce: Dispersal, postfire establishment, and growth in a warming climate, Ecol. Monogr., 78, 489–505, doi:10.1890/07-0074.1, 2008.

Woodard, P. M. and Delisle, G. P.: Biomass Regression Equations for Common Tree Seedlings and Shrubs in Jasper National Park, Alberta, University of Alberta Forestry Note 1, 1987.

Youngblood, A.: Development patterns in young conifer-hardwood forests of interior Alaska, J. Veg. Sci., 6, 229–236, doi:10.2307/3236218, 1995.

Zasada, J. C.: Effect of cone storage method and collection date on Alaskan white spruce (Picea glauca) seed quality, Proceedings of the International Symposium on Seed Processing, IUFRO, Bergen, Norway, 1973.

Zasada, J. C.: Case history of an excellent white spruce cone and seed crop in interior Alaska: Cone and seed production, germination, and seedling survival, US Forest Service General Technical Report PNW-65, Portland, OR, 1978.

Zasada, J. C.: Production, dispersal, and germination of white spruce and paper birch and first-year seedling establishment after the Rosie Creek fire., in: Early Results of the Rosie Creek Fire Reserach Project, edited by: Juday, G. and Dyrness, C. T., University of Alaska-Fairbanks Agriculture and Forestry Experiment Station Miscellaneous Publicatoin 85-2, 34–37, 1985.